

1 8 APR 2000

# Aging Aircraft NDE with Micromachined Ultrasonic Air Transducers

Final Report

for the period

March 1, 1999 to September 30, 1999

Air Force  
F49620-99-1-0137

G. L. Report No. 5700

Principal Investigator

B. T. Khuri-Yakub

Edward L. Ginzton Laboratory  
Stanford University  
Stanford, California 94305-4085

April. 2000

DTIC QUALITY INSPECTED 1

20000526 019

# REPORT DOCUMENT PAGE

AFRL-SR-BL-TR-00-

ring  
in of  
Suite

Public reporting burden for this collection of information is estimated to average 1 hour per response, including the time for reviewing the data needed, and completing and reviewing the collection of information. Send comments and suggestions for reducing this burden to Washington Headquarters Services, Directorate for Information Operations and Reports, 1204, Arlington, VA 22202-4302, and to the Office of Management and Budget, Paperwork Reduction Project (07-0302), Washington, DC 20503.

0186

1. AGENCY USE ONLY (Leave blank)

2. REPORT DATE  
12 April 003. REPORT TYPE AND DATES COVERED  
Final 01 Mar 99 - 30 Sep 99

4. TITLE AND SUBTITLE

AGING AIRCRAFT NDE WITH MICOMACHINED  
ULTRASONIC AIR TRANSDUCERS

5. FUNDING NUMBERS

2306/AX  
F49620-99-1-0137

6. AUTHORS

Butrus T. Khuri-Yakub

7. PERFORMING ORGANIZATION NAME(S) AND ADDRESSES

Edward L. Ginzton Laboratory  
Stanford University  
Stanford, CA 94305-40858. PERFORMING ORGANIZATION REPORT  
NUMBER9. SPONSORING / MONITORING AGENCY NAME(S) AND  
ADDRESS(ES)AFOSR/NA  
801 N. Randolph St. Room 732  
Arlington, VA 22203-197710. SPONSORING / MONITORING AGENCY  
REPORT NUMBER

G.L. 5700

11. SUPPLEMENTARY NOTES

12a. DISTRIBUTION / AVAILABILITY STATEMENT

Approved for public release:  
Distribution unlimited.

12b. DISTRIBUTION CODE

13. ABSTRACT (Maximum 200 words)

Due to the large impedance mismatch between common piezoelectric materials and air, conventional piezoelectric transducers are not very efficient sources of ultrasound in air. Therefore, piezoelectric nondestructive evaluation (NDE) systems must use a coupling fluid to improve the power transfer to the sample. Use of a coupling fluid or immersion of the sample complicates inspection, and in some cases is undesirable. Air-coupled ultrasonic systems are preferable as long as efficient transducers are available for transferring ultrasound into air. This report discusses some capacitive micromachined ultrasonic transducers (CMUTs) that have more than 100 dB dynamic range in a bistatic transmission system. These transducers consist of thousands of 1 (m-thick silicon-nitride membranes, resonating at 2-3 MHz electrically connected in parallel. Equivalent circuit modeling of the transducers provides insight into the design of the devices and enables accurate predictions of CMUTs' behavior in NDE systems. Finally, the report concludes with some discussion of current research in developing efficient, wide-band CMUTs.

14. SUBJECT TERMS

Transducer, Air, Capacitive, NDE, CMUT

15. NUMBER OF PAGES

7

16. PRICE CODE

17. SECURITY CLASSIFICATION  
OF REPORT  
UNCLASSIFIED18. SECURITY CLASSIFICATION  
OF THIS PAGE  
UNCLASSIFIED19. SECURITY CLASSIFICATION  
OF ABSTRACT  
UNCLASSIFIED

20. LIMITATION OF ABSTRACT

# Aging Aircraft NDE with Micromachined Ultrasonic Air Transducers

## 1. INTRODUCTION

Conventional methods of ultrasonic nondestructive evaluation (NDE) use liquids to couple sound waves into the test sample. This either requires immersion of the parts to be examined or the use of complex and bulky water squirting systems that must be scanned over the structure. An alternative is to place the transducer in direct contact with the samples under test.<sup>1</sup> However, defect detection or imaging can be time consuming, and fragile samples may be damaged by direct contact. In such situations, air borne ultrasound is a useful non-contact method of detecting and imaging, given efficient and sensitive transducers for use as transmitters and receivers.

Most ultrasonics research of the past century has focused on piezoelectric transducers for transmission and reception of ultrasound to and from liquids and solids. Although piezoelectric transducers have found numerous applications to ultrasound in solids and liquids, they are relatively inefficient sources of ultrasound in air, largely due to the tremendous impedance mismatch between piezoelectric materials and air. The acoustic impedance of air at standard temperature and pressure is 427 rayls (mks units  $\text{kg/m}^2\text{-sec}$ ) while piezoelectrics, like nearly all solids and most liquids, have acoustic impedances on the order of  $10^6$  to  $10^7$  rayls<sup>2</sup>. While it is possible to improve the impedance match using matching layers, few low-loss materials exist which have impedances between those of solids and gases, and the necessary layer thicknesses may be too thin to realize in practice.<sup>3</sup> In addition, improvements in efficiency due to matching come at the expense of bandwidth, since matching layers are only a quarter wavelength at one frequency.

Recently, several capacitive micromachined ultrasonic transducers (CMUTs) have been developed, which are capable of efficient excitation and detection of ultrasound in air<sup>4,5</sup>. The membrane structure of a CMUT, or any basic capacitive transducer design is shown in Fig. 1.

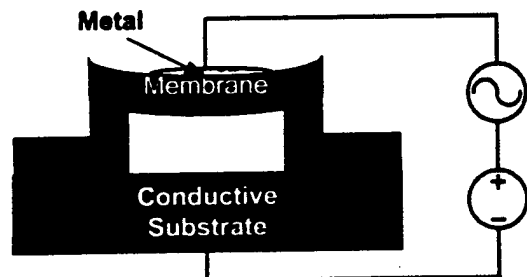


Fig. 1. Structure of a single membrane.

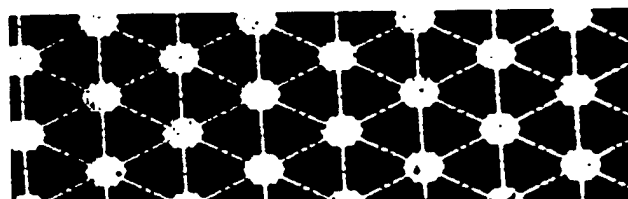


Fig. 2. Magnified view of CMUT with hexagonal close-packed membranes.

A CMUT transducer consists of a several thousand such membranes electrically connected in parallel to form a 1 cm by 1 cm transducer, a section of which is shown in Fig. 2. When the membranes are biased with a DC bias voltage, AC voltage excitations generate pressure waves in the air. Reception of ultrasound by the same device is analogous, as the impinging sound pressure moves the membrane, modulating the voltage (or alternatively, the charge) on the membrane.

## 2. CMUT FABRICATION

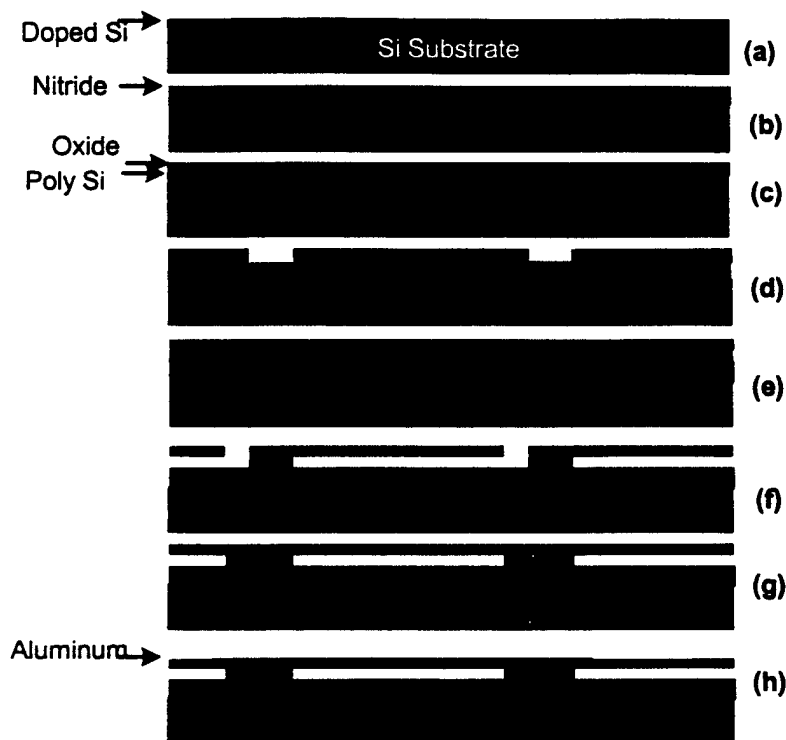


Fig. 3. Schematic diagram showing relevant steps in process flow for CMUT.

CMUT devices have been reliably fabricated for several years at the Stanford Nanofabrication Facility (SNF), Stanford, CA, by students of Professor Khuri-Yakub. The basic process flow for the CMUT is shown schematically in Fig. 3. First, a silicon substrate is doped to form the conductive lower plate of the capacitor (a). An insulating layer of nitride is deposited over the substrate (b). Several sacrificial layers are deposited and subsequently patterned by photolithography to defined the lateral membrane dimensions (c and d). A conformal silicon-nitride deposition forms the transducer membranes (e). The membrane is released from the substrate by etching a sacrificial layer through tiny via holes (f). These via holes may be subsequently vacuum-sealed for immersion applications. Finally, aluminum is patterned on the membranes to form the upper electrodes for the capacitive membranes. CMUTs can be

reliably micromachined due to the excellent precision, resolution, and repeatability of the standard semiconductor processing techniques used in fabrication.

## 3. THEORY AND MODELING OF CMUTS

### 3.1. Theory of Operation

Referring again to the structure of a single membrane, the electrostatic force actuates the membrane by attracting it toward the substrate. A restoring spring force is generated due to some combination of tension in the flexed membrane and squeeze film effects of the air between the membrane and substrate, depending on the design. Because the electrostatic force is always attractive, the transducer must be used with a bias voltage so that small deflections in displacement generate restoring spring forces. Of course, any dynamical equation of motion must also consider the mass of the membrane that is accelerated under these opposing forces. Thus, it appears as if the capacitive transducer is a damped mass-spring system actuated with electrostatic force. Although the static deflection of the device under a DC voltage bias is well-understood and modeled,<sup>6</sup> the full-dynamics of the CMUT under AC excitation are quite complicated. Since the electrostatic force and restoring forces are non-linear functions, the motion of the membrane is governed by non-linear differential equations. Therefore, it is useful to make some simplifying assumptions to gain some practical insight into the design and

application of the device. Much like transistor small-signal analysis, an equivalent small-signal circuit can be derived for AC analysis around a DC operating point, set by the bias voltage on the membrane. Such analysis is accurate as long as the membrane displacement under AC excitation is a small fraction of the membrane deflection under a DC bias voltage.

### 3.2. Transducer Circuit Models

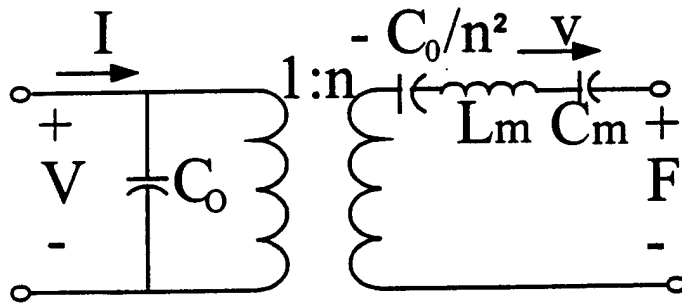


Fig. 4. Equivalent two-port network of CMUT membrane.

The derivation of a small-signal circuit model facilitates analysis of the transducer since circuit theory can be leveraged for understanding. The circuit is best modeled as a lumped two-port network that relates electrical and mechanical analogues such as voltage and current to force and velocity. A derivation of the equivalent circuit model for a single CMUT membrane, shown in Fig. 4, is performed by Ladabaum.<sup>6</sup> In

Fig. 4, voltage and current on the left of the figure, are transformed through an ideal transformer, with a turns ratio of  $n$ , into force and velocity. The membrane capacitance is given by  $C_0$  and the membrane impedance,  $Z_m$ , is well-approximated by a series inductor-capacitor (LC) circuit of values  $L_m$  and  $C_m$ , as suggested by Mason.<sup>7</sup> The actual impedance of the membrane, derived by Mason, shows the dependence of the membrane impedance on processing parameters such as material constants and dimensions:

$$Z_m = j\omega\rho\ell_1 S \left[ \frac{\ell_1 a k_1 k_2 (k_2 I_1(k_2 a) J_0(k_1 a) + \ell_1 k_1 J_1(k_1 a) I_0(k_2 a))}{a k_1 k_2 (k_2 I_1(k_2 a) J_0(k_1 a) + k_1 J_1(k_1 a) I_0(k_2 a) - 2(k_1^2 + k_2^2) J_1(k_1 a) I_1(k_2 a))} \right]$$

where  $k_1 = \sqrt{\frac{\sqrt{d^2 + 4c\omega^2} - d}{2c}}$ ,  $k_2 = \sqrt{\frac{\sqrt{d^2 + 4c\omega^2} + d}{2c}}$ ,  $c = \frac{\ell_1^2 (Y_0 + T_n)}{12(1 - \sigma^2)}$ , and  $d = \frac{T_n}{\rho}$ .

This equation shows the dependence on membrane radius ( $a$ ), tension ( $T_n$ ), thickness ( $\ell_1$ ), density ( $\rho$ ), Poisson's ratio ( $\sigma$ ), steady-state frequency ( $\omega$ ), area ( $S$ ), and Young's modulus ( $Y_0$ ). Examination of this expression shows why CMUT membranes must be small, thin, and light. Micromachining these membranes reduces the mechanical impedance, improving the power that is delivered to the air impedance. The same equivalent circuit elements of Fig. 4 can describe a transducer that has thousands of piston-like membranes in moving in parallel by adjusting some of the circuit element values by constant factors.

When the CMUT is operating in air, the right terminals of Fig. 4 are connected to a largely real resistance, which represents the radiation impedance into air. The membrane losses, both structural and due to squeeze-film damping, can also be approximated by a real impedance. The circuit model of Fig. 5 results from transformation of the mechanical parameters to the electrical side of the circuit.

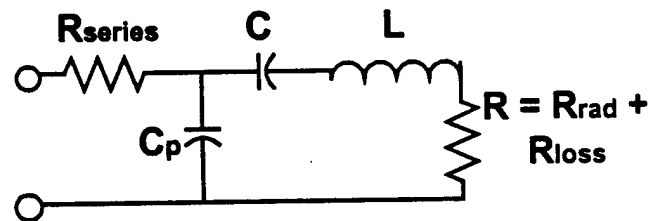


Fig. 5. Electrical circuit model of CMUT operating in air.

### 3.3. Characterization of CMUTs

We have developed several test and measurement configurations for evaluation of transducers and comparison to the circuit models. First, input impedance measurements of a CMUT in air, using a network analyzer, permit a curve-fit of the equivalent circuit model shown in Fig. 5. Figure 6 shows one such curve-fit of a transducer and the corresponding element values.

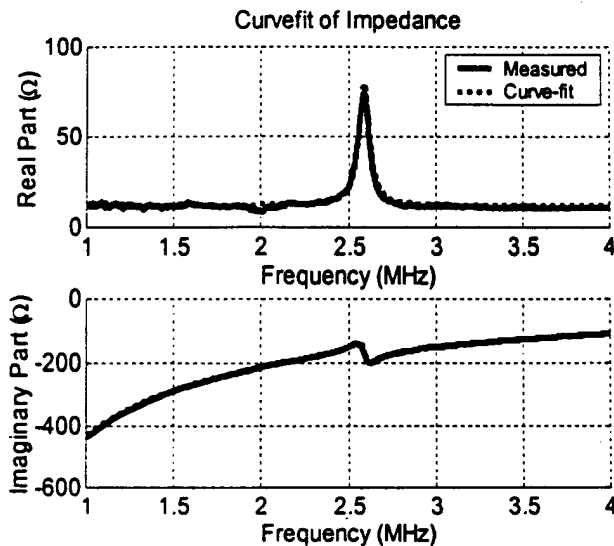


Fig. 6. Curvefit of input impedance data using element values:  $R = 420 \Omega$ ,  $C = 4.0 \text{ pF}$ ,  $L = 946 \mu\text{H}$ ,  $C_p = 365 \text{ pF}$ , and  $R_{\text{series}} = 12 \Omega$ .

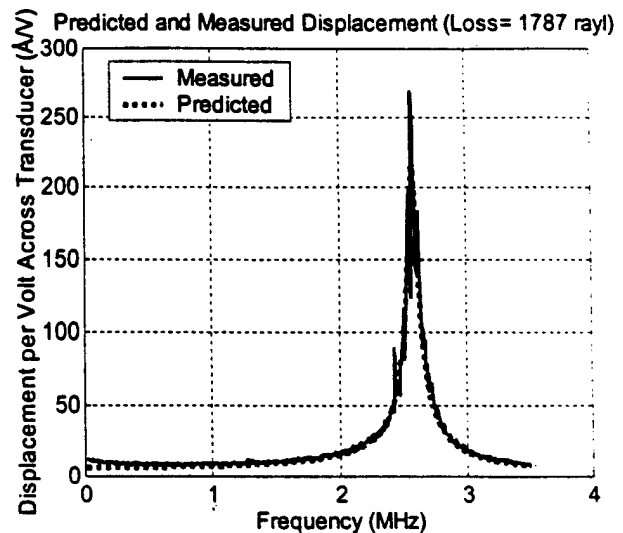


Fig. 7. Measured and predicted membrane displacement based on circuit model.

Similar measurements of impedance in vacuum permit distinction of losses into structural and air-damping categories. At present the structural losses are very small, comprising approximately 5 % of the total loss when operating in air.

Measurement of membrane displacement using a laser interferometer is another useful characterization tool, particularly for finding the ratio of radiation impedance to loss impedance for each membrane. Figure 7 compares the predicted and measured displacement for the same transducer using the element values found by curve-fitting the impedance and The transformer turns ratio of Fig. 4 can also be calculated from the data, which allows direct comparison of the transducer's mechanical characteristics to those predicted by theory. Displacement measurements on individual membranes of a CMUT also permit tracking of process variations between membranes in the same transducer, which aids in improving CMUT design and fabrication procedures.

## 4. TRANSDUCER CONSIDERATIONS FOR AIR APPLICATIONS

### 4.1. Dynamic Range

Because any air-coupled NDE system must tolerate severe signal attenuation at the interfaces between air and the solid sample under inspection, dynamic range is a primary concern in the design of CMUTs. Although dynamic range is highly dependent on the impedance and noise characteristics of the supporting electronics in the system, it is also highly dependent on the efficiency of the transducers used for sending and receiving ultrasound.

Dynamic range of a pitch-catch system of two CMUTs is simply measured as the received signal-to-noise ratio (SNR), with adjustments for any attenuation suffered by the signal in the medium. Thus, dynamic range is defined here as the maximum amount of attenuation that can be tolerated over the

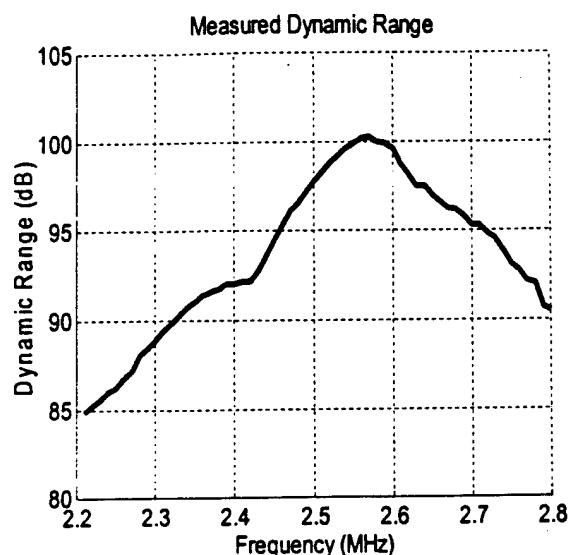


Fig. 7. Measured dynamic range of system using two similar CMUTs in pitch-catch configuration in air.

noise in a transmit-receive system. Using a commercially available amplifier, the AD600 with 1.4 nV/ $\sqrt{\text{Hz}}$  noise voltage, and measuring over a generous 2 MHz noise bandwidth, the dynamic range of the pitch-catch CMUT system regularly surpasses 100 dB, as shown in one such measurement in Fig. 8. This dynamic range is sufficient to image defects in solids using two transducers in through transmission or through excitation and through excitation and detection of guided lamb waves in a single-sided inspection system.<sup>8</sup>

The insertion loss of a transducer can be characterized through a pitch-catch transducer configuration involving two similar transducers, face-to-face. Measurements suggest that the insertion loss is approximately 20 dB, though the value varies significantly with transducer design and processing. The primary source of loss in the CMUT is the squeeze-film damping due to air behind the membrane. Such losses could be reduced by vacuum

sealing the space behind the membrane, as is regularly done with CMUTs for immersion applications. However, reducing the loss in the transducer also reduces its bandwidth.

#### 4.2. Bandwidth

A second consideration for air-coupled NDE applications, which is often at odds with efficiency, is bandwidth. Large bandwidth not only permits use of various ultrasonic frequencies in a single device, but more importantly allows the transducer to reach its maximum displacement in fewer cycles. This is particularly important if the transducers are to be used in a pulse-echo configuration for single-sided inspection. The ability to excite a transducer with a short tone burst defines the depth of field for of the device, since the receiver must temporally resolve the ultrasound echoes from various depths in the sample. Large bandwidth is easily obtained by introducing some loss mechanisms into the transducer. However, bandwidth obtained in this way comes at the expense of dynamic range and efficiency, and thus limits the range of suitable NDE applications.

### 5. CURRENT RESEARCH

Current research is underway to develop a CMUT that is both efficient and wide-band when operating in air. One way to obtain bandwidth without introducing additional loss to the transducer is shown schematically in Fig. 8. This transducer has membranes of various dimensions connected in parallel to form the CMUT. . A rectangular, rather than circular, membrane allows closer packing of membranes of different sizes. Because each membrane size corresponds to a particular resonant frequency, the various membranes in parallel broaden the overall frequency response of the CMUT.

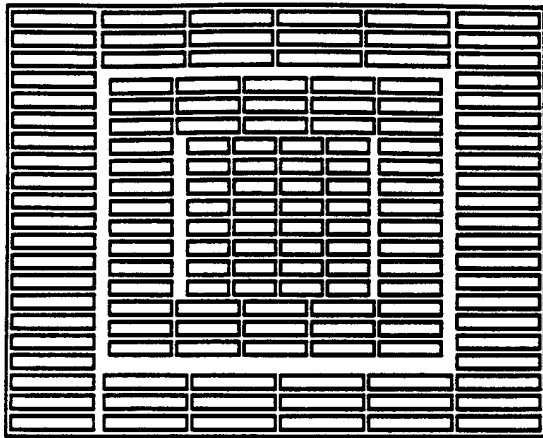


Fig. 8. Depiction of broadband CMUT comprised of membranes with varying dimensions (actual design has thousands of membranes).

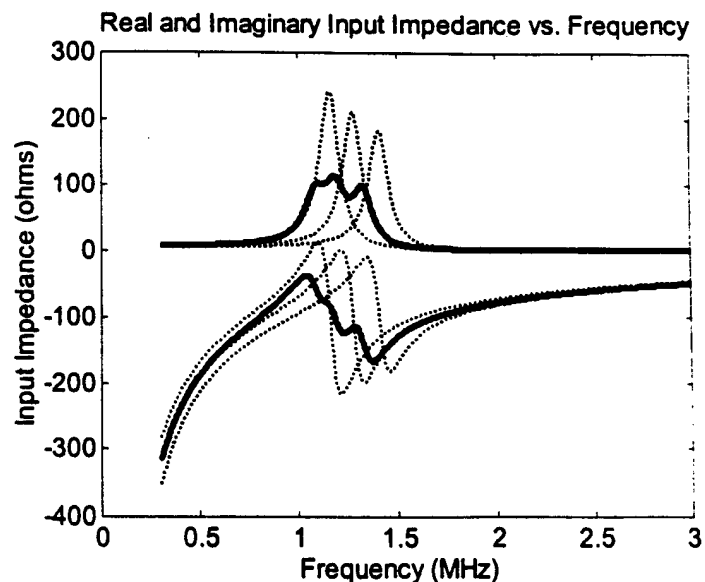


Fig. 9. Predicted input impedance of broadband CMUT (solid line) compared to input impedances of CMUTs with uniform membrane size (dotted lines).

Because the individual membranes retain their highly resonant structure with low-losses, efficiency is not sacrificed in this design. Figure 9 shows the predicted input impedance of such a device with three different membrane sizes. The dotted lines show the predicted input impedance of a comparable CMUT made up of only one membrane size. The real part of the composite input impedance is noticeably wider than the individual resonance peaks. This concept of combining membranes of non-uniform dimensions can obviously be extended until a continuum of sizes and resonant frequencies is included, resulting in a broadband device.

The fabrication steps for CMUTs with varying membrane dimensions remain nearly identical to those of the previous single-size CMUT devices, though new photolithography masks are necessary. We have produced masks for the broadband CMUT device depicted in Fig. 8. Fabrication of these devices is presently underway at SNF. Once fabrication is complete, we plan to characterize the devices using membrane displacement measurements, input impedance measurements, and system characterization of bandwidth and dynamic range in pitch-catch and pulse-echo configurations.

- <sup>1</sup> F. L. Degertekin and B. T. Khuri-Yakub, "Hertzian contact transducers for non destructive evaluation," *J. Acoust. Soc. Amer.* **99**, pp. 299-308, 1996.
- <sup>2</sup> G. Kino, *Acoustic Waves: Devices, Imaging, and Analog Signal Processing*, Prentice Hall, Englewood Cliffs, 1987.
- <sup>3</sup> M. I. Haller, "Micromachined Ultrasonic Devices and Materials," PhD Thesis, Stanford University, Stanford, CA, May 1998.
- <sup>4</sup> M. I. Haller and B. T. Khuri-Yakub, "A surface micromachined electrostatic ultrasonic air transducer," *IEEE Trans. On Ultrasonics, Ferroelectrics and Frequency Control* **43**, pp.1-6, 1996.
- <sup>5</sup> D. W. Schindel and D. A. Hutchins, "Applications of micromachined capacitance transducers in air-coupled ultrasonics and nondestructive evaluation," *IEEE Trans. On Ultrasonics, Ferroelectrics and Frequency Control* **42**, pp. 51-58, 1995.



- 
- <sup>6</sup> I. Ladabaum, X. C. Jin, H. T. Soh, A. Atalar, and B. T. Khuri-Yakub, "Surface micromachined capacitive ultrasonics transducers," *IEEE Trans. On Ultrasonics, Ferroelectrics and Frequency Control* **45**, pp. 678-690, 1998.
- <sup>7</sup> W. P. Mason, *Electromechanical Transducers and Wave Filters*, Van Nostrand, New York, 1948.
- <sup>8</sup> S. Hansen, F. Levent Degertekin, and B. T. Khuri-Yakub, "Micromachined Ultrasonic Transducers for Air-Coupled Non-Destructive Evaluation," *Proceedings of SPIE* **3586**, pp. 310-318, 1999.

### **Personnel Supported**

B. T. Khuri-Yakub (Faculty)  
S. Hansen (Graduate Student)

### **Publications**

None